

2

PL-TR-92-2113

**AD-A261 750**



**DIGITAL OBLIQUE REMOTE IONOSPHERIC SENSING (DORIS)  
PROGRAM DEVELOPMENT**

Walter Kuklinski  
John Hazelwood  
Bodo W. Reinisch

University of Massachusetts Lowell  
Center for Atmospheric Research  
450 Aiken Street  
Lowell, Massachusetts 01854



April 1992

Scientific Report #5

Approved for public release; distribution unlimited.



PHILLIPS LABORATORY  
AIR FORCE SYSTEMS COMMAND  
HANSCOM AIR FORCE BASE, MA 01731-5000


**93-02160**



This technical report has been reviewed and is approved for publication.

  
JURGEN BUCHAU  
Contract Manager

  
JOHN E. RASMUSSEN, Chief  
Ionospheric Application Branch

  
WILLIAM K. VICKERY, Director  
Ionospheric Effects Division

This document has been reviewed by the ESD Public Affairs Office (PA) and is releasable to the National Technical Information Service (NTIS).

Qualified requestors may obtain additional copies from the Defense Technical Information Center. All others should apply to the National Technical Information Service.

If your address has changed, or if you wish to be removed from the mailing list, or if the addressee is no longer employed by your organization, please notify PL/TSI, Hanscom AFB, MA 01731-5000. This will assist us in maintaining a current mailing list.

Do not return copies of this report unless contractual obligations or notices on a specific document requires that it be returned.

# REPORT DOCUMENTATION PAGE

Form Approved  
OMB No. 0704-0188

Public reporting burden for this collection of information is estimated to average 1 hour per response, including the time for reviewing instructions, searching existing data sources, gathering and maintaining the data needed, and completing and reviewing the collection of information. Send comments regarding this burden estimate or any other aspect of this collection of information, including suggestions for reducing this burden, to Washington Headquarters Services, Directorate for Information Operations and Reports, 1215 Jefferson Davis Highway, Suite 1204, Arlington, VA 22202-4302, and to the Office of Management and Budget, Paperwork Reduction Project (0704-0188), Washington, DC 20503.

1. AGENCY USE ONLY (Leave blank)		2. REPORT DATE April 1992		3. REPORT TYPE AND DATES COVERED Scientific No. 5	
4. TITLE AND SUBTITLE Digital Oblique Remote Ionospheric Sensing (DORIS) Program Development				5. FUNDING NUMBERS PE 12417F PR ESDO TA 01 WU AB Contract F19628-90-K-0029	
6. AUTHOR(S) Walter Kuklinski Jon Hazelwood Bodo W. Reinisch					
7. PERFORMING ORGANIZATION NAME(S) AND ADDRESS(ES) University of Massachusetts Lowell Center for Atmospheric Research 450 Aiken Street Lowell, MA 01854				8. PERFORMING ORGANIZATION REPORT NUMBER	
9. SPONSORING/MONITORING AGENCY NAME(S) AND ADDRESS(ES) Phillips Laboratory Hanscom AFB, MA 01731-5000  Contract Monitor: Jurgen Buchau/GPIS				10. SPONSORING/MONITORING AGENCY REPORT NUMBER  PL-TR-92-2113	
11. SUPPLEMENTARY NOTES					
12a. DISTRIBUTION/AVAILABILITY STATEMENT Approved for public release; distribution unlimited				12b. DISTRIBUTION CODE	
13. ABSTRACT (Maximum 200 words)  The development and performance of a complete oblique ionogram autoscaling and inversion algorithm is presented. The inversion algorithm uses a three layer quasiparabolic model of the midpoint electron density profile. The inversion process is formulated as an optimization problem that uses a two-stage simulated annealing optimization algorithm. The inversion algorithm was tested using both synthetic data and oblique ionogram data obtained for a link between Goose Bay and Wallops Island. The results of the inversion were compared with midpoint electron density profiles recorded at the Maine OTH radar.					
14. SUBJECT TERMS Oblique Propagation; Oblique Ionogram Autoscaling; Electron Density Profile Inversion; Simulated Annealing Optimization				15. NUMBER OF PAGES 46	
				16. PRICE CODE	
17. SECURITY CLASSIFICATION OF REPORT Unclassified	18. SECURITY CLASSIFICATION OF THIS PAGE Unclassified	19. SECURITY CLASSIFICATION OF ABSTRACT Unclassified	20. LIMITATION OF ABSTRACT SAR		

# TABLE OF CONTENTS

	Page
1.0 INTRODUCTION .....	1
2.0 REVIEW OF OBLIQUE IONOGRAM NOISE AND SUPPRESSION AND AUTOSCALING ALGORITHM.....	2
3.0 MODIFICATIONS AND IMPROVEMENTS MADE TO INVERSION ALGORITHM.....	5
4.0 RESULTS.....	8
5.0 STATUS OF EXISTING PROCESSING SOFTWARE.....	13
6.0 CONCLUSIONS .....	14
7.0 REFERENCES .....	15
Appendix A.....	17
Appendix B.....	32

<b>Accession For</b>	
NTIS GRA&I	<input checked="" type="checkbox"/>
DTIC TAB	<input type="checkbox"/>
Unannounced	<input type="checkbox"/>
Justification	
By	
Distribution/	
Availability Codes	
Dist	Avail and/or Special
A-1	

## LIST OF FIGURES

Figure No.		Page
1	Two-Dimensional Wiener Filtering.....	4
2	Algorithm Iterative Procedure.....	6
3	Synthetic Oblique Ionogram.....	9
4	Inversion Using Data from Figure 3.....	10
5	Oblique Ionogram Goose Bay - Wallops.....	11
6	Inversion Using Data from Figure 5.....	12

## 1.0 INTRODUCTION

Ionospheric mapping and modeling relies on measured ionospheric characteristics. The U.S. Air Force DISS (Digital Ionospheric Sounding Systems) network of ionosondes provides real time electron density profiles for the locations of the sounders. Valuable additional information can be obtained for the ionospheric mid-points between two stations separated by 1000 to 3000 km by the use of oblique ionograms. Since the Digisonde 256 sounders used in the DISS network are capable to operate in the oblique ionogram mode, the Phillips Laboratory initiated the DORIS (Digital Oblique Remote Ionospheric Sensing) program in 1987 to establish the feasibility of such an approach.

In a number of reports, the University of Massachusetts Lowell, Center for Atmospheric Research (ULCAR) documented the system requirements, test data, and results of oblique sounding between existing DISS modes (Kuklinski et al., 1987). Operational implementation of the DORIS technique relies on the development of software that automatically inverts the oblique ionograms into mid-point electron density profiles. The inversion from oblique ionogram to mid-point profile (DORIS inversion) consist of two major sections of about equal difficulty: one, the autoscaling and identification of the various echo traces, and two, the inversion of the trace into a representative mid-point electron density profile. The autoscaling section was described by Kuklinski et al., (1992). The present report describes an innovative inversion technique.

During the period 30 April 1990 through 31 September 1992, ULCAR implemented and tested a complete oblique ionogram autoscaling and inversion algorithm using both synthetic and actual oblique ionogram data. The DORIS program uses a three layer quasiparabolic model to represent the midpoint electron density profile. The inversion process was formulated as a two stage configurational optimization problem, that was solved using a simulated annealing optimization technique. Results of this work were reported in a paper (Reinisch et al., 1991) and presented at the AGARD Conference in Turkey in October 1991. This paper is attached in Appendix

A to this report. Section 2 reviews some of the work reported earlier (Kuklinski et al., 1988, 1989, 1990).

## 2.0 REVIEW OF OBLIQUE IONOGRAM NOISE SUPPRESSION AND AUTOSCALING ALGORITHM

The automatic oblique ionogram noise suppression and scaling algorithms use a scaled vertical ionogram, produced by the Digisonde ARTIST (Reinisch, et al., 1989), to synthesize the echo traces that would be measured over the oblique link if the midpoint ionosphere and the ionosphere at the transmitter were identical. These synthesized oblique echo traces are used by the subsequent noise suppression filter and the trace identification algorithm.

The first operation performed on the received oblique ionogram is a frequency redundancy noise suppression. A 100 kHz oblique ionogram is generated from either 25 or 50 kHz sounding data by selecting the highest signal-to-noise ratio channel from each set of four adjacent 25 kHz soundings or two adjacent 50 kHz soundings. The effectiveness of this technique is based on the fact that the interfering signals produced by spurious radio transmitters are manifested as large amplitude signals at every group path for a narrow frequency band; generally an interfering transmitter appears at only one sounding frequency. Since the group path is essentially constant, that is it changes less than the resolution of the measurement technique (5 km), for several 25 or 50 kHz sounding frequencies, the individual sounding frequency with the highest signal to noise ratio within a predetermined frequency range can be used to represent that entire range.

The subsequent noise suppression filter uses a minimum-mean-square Wiener filtering technique. The preprocessed 100 kHz ionogram is modelled as the sum of a noise/interference signal and a desired noise free oblique ionogram. The filter is obtained by dividing the power spectral density of the synthesized oblique echo traces by the sum of the power spectral densities of the synthesized oblique echo traces and an estimate of the noise. The noise estimate is calculated from the average of a large number of

ionograms obtained with the receiver subsystem operating, but with the transmitter off. The 2-D Fourier transform of the preprocessed 100 kHz ionogram is multiplied by the resulting Wiener filter. The inverse 2-D Fourier transform of the resulting product produces the potential oblique echo trace segments. This process is outlined in Figure 1.

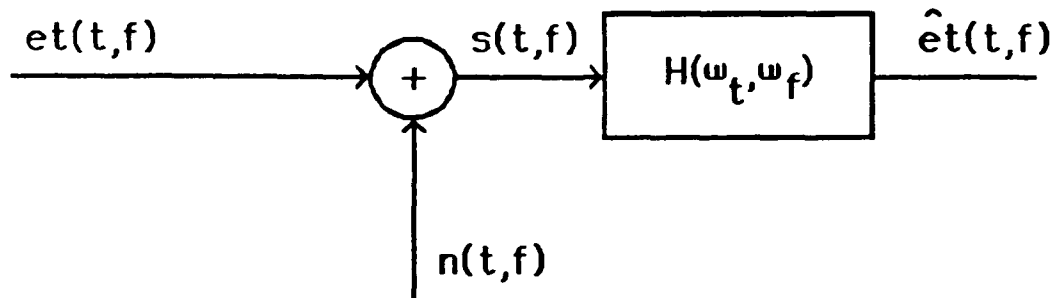
The synthesized oblique echo traces, derived from the ARTIST scaled vertical data, are used to define regions of interest for subsequent processing of the potential oblique echo traces. These regions of interest are defined as all points within a fixed number of range bins and sampling frequencies of the synthesized oblique echo traces. At present the allowable variations were derived from the variances of an oblique ionogram data base. Any data in the region of interest for a particular layer is considered to be a potential part of the echo trace for that layer.

The echo trace segments in a particular region of interest are scaled using a tracking algorithm. This algorithm takes and finds the best fit of a template of the echo trace cross-section to an initial point on the echo trace segment. To obtain the best fit, the template is translated and rotated about the initial point. The results of the fitting process are the locations of the center, leading and trailing edges of the echo trace. The algorithm uses these points to determine the next point on the echo trace where the template fitting procedure is repeated. The entire echo trace is tracked in this manner.

The leading edge points determined by the tracking algorithm are used to determine the parameters of a three layer quasiparabolic electron density profile model.



Oblique Ionogram:  $s(t,f) = n(t,f) + et(t,f)$



Assumptions:  $n(t,f)$  Stationary Random Process of  
Known PSD =  $P_n(\omega_t, \omega_f)$

$et(t,f)$  Stationary Random Process of  
Known PSD =  $P_{et}(\omega_t, \omega_f)$

$$H(\omega_t, \omega_f) = \frac{P_{et}(\omega_t, \omega_f)}{P_{et}(\omega_t, \omega_f) + P_n(\omega_t, \omega_f)}$$

Result:  $\hat{et}(t,f)$  MMSE Estimate of  $et(t,f)$

Figure 1. Two-Dimensional Wiener Filtering

### 3.0 MODIFICATIONS AND IMPROVEMENTS MADE TO INVERSION ALGORITHM

The most significant modification of the previously proposed inversion algorithm is the utilization of a simulated annealing optimization technique to perform the inversion process. A major limitation of the previously proposed inversion process, in particular for long ground ranges and multiple layer data, was the numerical stability of the iterative Newton-Raphson technique. An additional limitation of this technique was that while, in principle, each layer could be described by more than one quasiparabolic segment, no straight forward technique was available to determine the optimum number of segments for any given scaled echo trace. Typically the optimum will be a compromise between a single quasiparabolic layer, which may not adequately describe the actual layer, and a large number of quasiparabolic segments, which yield a numerically unstable inversion problem. The formulation of the inversion problem as a configurational optimization problem allowed a simulated annealing technique that yielded the desired optimal representation of each layer, to be used (Dyson and Bennett, 1988).

An additional change that was made to the inversion algorithm was the inclusion of a two-stage inversion algorithm that iteratively adjusted the quasiparabolic layer parameters to satisfy the observed propagation mode extremes before the final simulated annealing optimization technique was applied. The two-stage inversion algorithm was implemented by the addition of an iterative procedure, outlined in Figure 2. This procedure was applied in sequence to the E, F1 and F2 layers. For each layer an estimate of the QP layer parameters were obtained from either a scaled vertical end-point ionogram and/or an ionospheric model. These initial estimates are labeled  $y_m^0$ ,  $r_h^0$  and  $f_c^0$  in the upper panel of

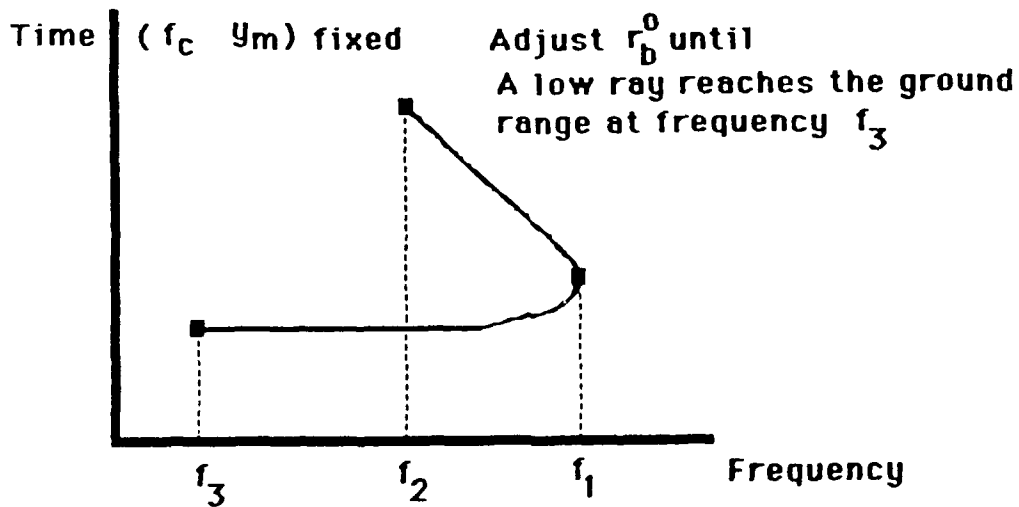
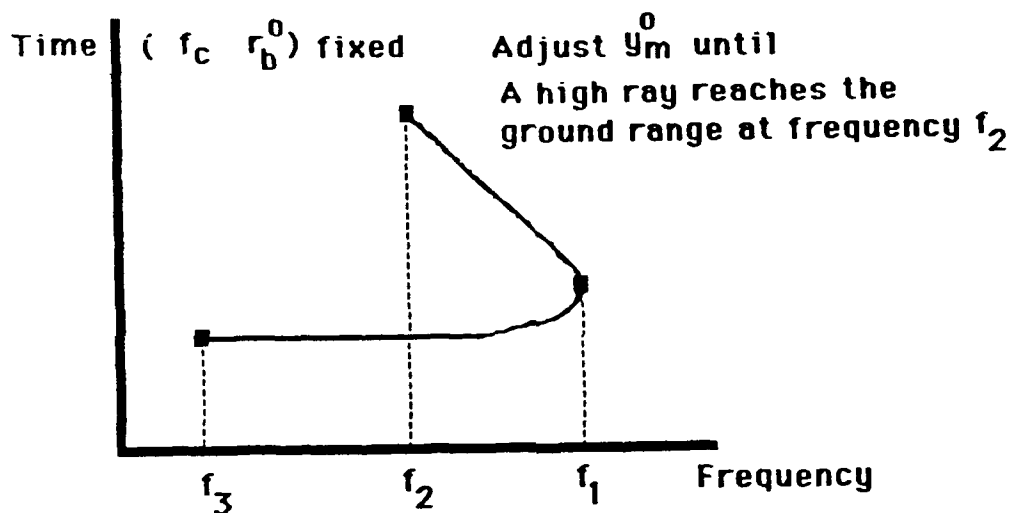
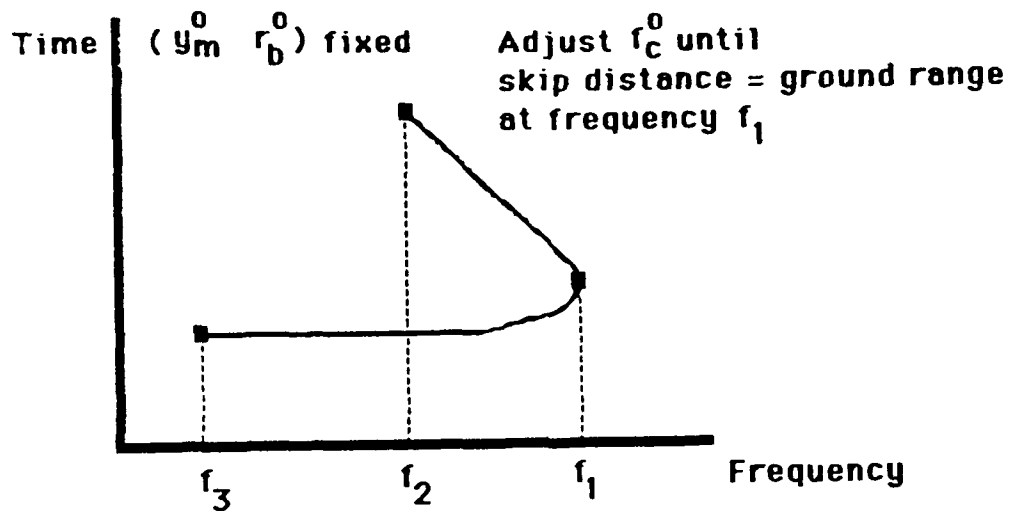


Figure 2. Algorithm Iterative Procedure

Figure 2 which shows the iterative procedure for a single layer. In Figure 2,  $f_1$  is the MUF frequency,  $f_2$  the lowest frequency where a high ray propagation mode was observed in the oblique ionogram and  $f_3$  the lowest frequency where a low ray propagation mode was observed in the oblique ionogram. The procedure adjusted the critical frequency of the layer until no ray reached the known ground range for any frequencies above the observed MUF frequency, as seen in the upper panel of Figure 2; adjusted the semithickness of the layer until at least one high-angle ray reached the known ground range at the lowest observed high-angle ray sounding frequency as seen in the middle panel of Figure 2; and adjusted the base height of the layer until at least one low-angle ray reached the known ground range at the lowest observed low-angle ray sounding frequency, as seen in the lower panel of Figure 2. This sequence of adjustments was repeated until all three of the observed propagation mode extremes were simultaneously satisfied. This initial "coarse" inversion process was tested using the Wallops Island to Goose Bay oblique ionograms. In every case the procedure rapidly converged to a quasiparabolic layer model that produced group paths at all sounding frequencies that were within 50 km of the actual group paths. The subsequent simulated annealing optimization algorithm made "fine" adjustments in the layer parameters resulting in electron density profiles with critical frequencies within 200 kHz of the correct values and peak heights within 20 km of the correct values.

The simulated annealing optimization technique used an analogy between the configurational optimization problem of interest and the cooling of a thermodynamic system. The energy of a thermodynamic system that has been slowly cooled is minimum, while a quickly cooled system typically arrives at a higher final energy state. These are analogous to the desired global minimum and a local minimum, respectively, of the given configurational optimization problem. The simulated annealing technique avoids the local minima produced by most iterative optimization techniques that employ some type of gradient algorithm by allowing changes in configuration that may increase the desired cost function for some fraction of the iterations. The cost function that was minimized in the electron density inversion problem was the total squared error between the measured group path vs. sounding frequency data and the group path vs.

sounding frequency data produced by the quasiparabolic model. The configuration of the model consisted of the specific values of semithickness, peak height and critical frequency for each layer.

#### 4.0 RESULTS

The completed inversion algorithm was first tested using synthetic data generated by the three layer quasiparabolic model analytic ray tracing software developed during this project. A typical synthetic oblique ionogram is seen in Figure 3. This ionogram was calculated for a ground range of 2060 km, the length of the Goose Bay to Wallops Island link used to produce actual oblique ionograms. The analytic ray tracing software determined both one and two hop propagation modes and identified echo trace points as either high or low ray modes. This identification is important during the simulated annealing optimization process. Since a complete QP electron density profile model for each layer allows propagation modes, for a given sounding frequency and ground range, an ambiguity can exist during the inversion process. By tugging each point on the oblique ionogram, the ambiguity is removed and the inversion process can be more efficient and accurate.

Using the echo trace points indicated with circular dots in Figure 3, the inversion algorithm produced the profile seen in Figure 4. The electron density used to generate the oblique ionogram and the electron density produced by the inversion algorithm are essentially identical.

Figures 5 and 6 illustrate the application of the DORIS algorithms to real data. Figure 5a shows a typical Goose Bay to Wallops Island oblique ionogram. The  $\pm$  symbols mark the autoscaled trace points. Figure 6 shows the midpoint electron density profile produced by the DORIS inversion algorithm together with the mid-point electron density profile determined from a simultaneous vertical ionogram recorded at the Maine

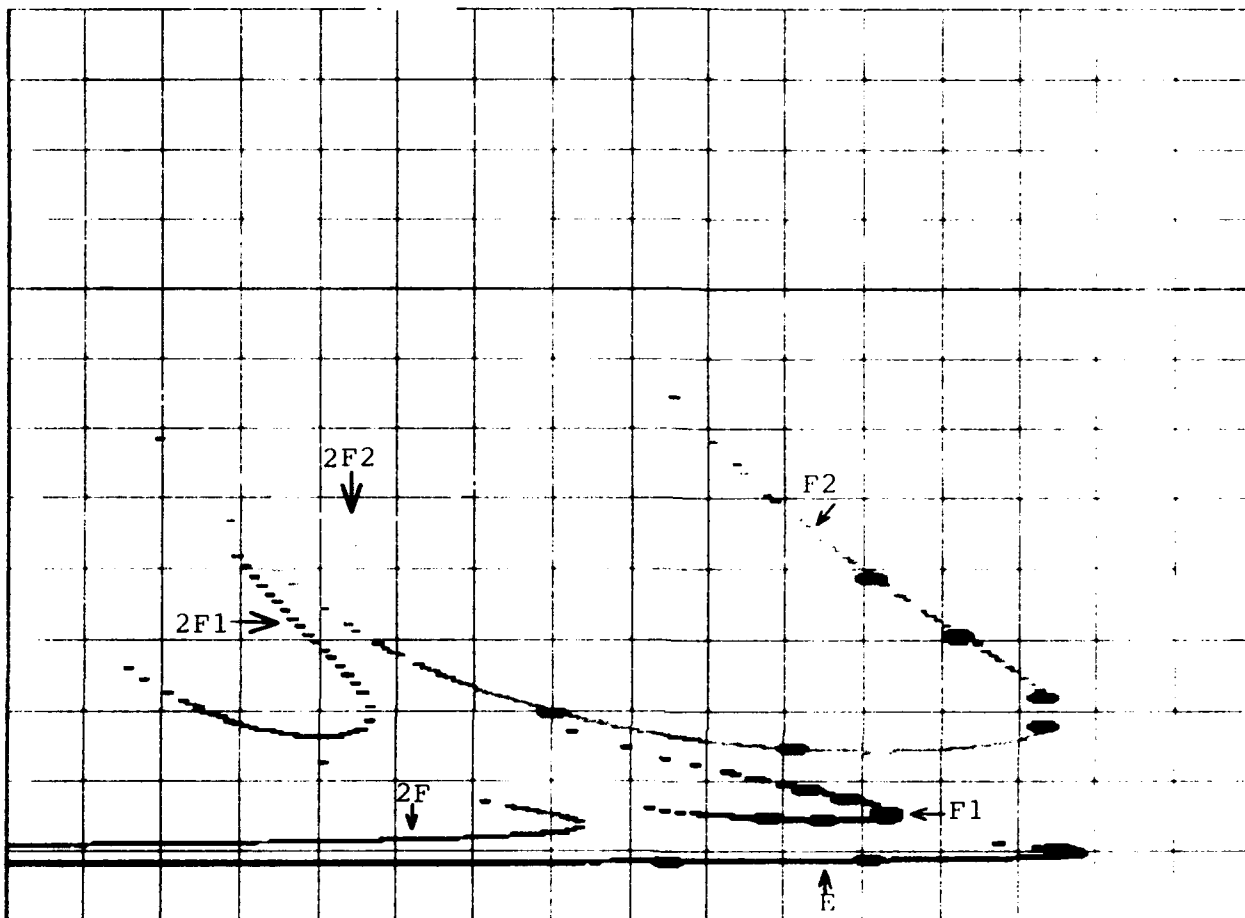


Figure 3. Synthetic Oblique Ionogram

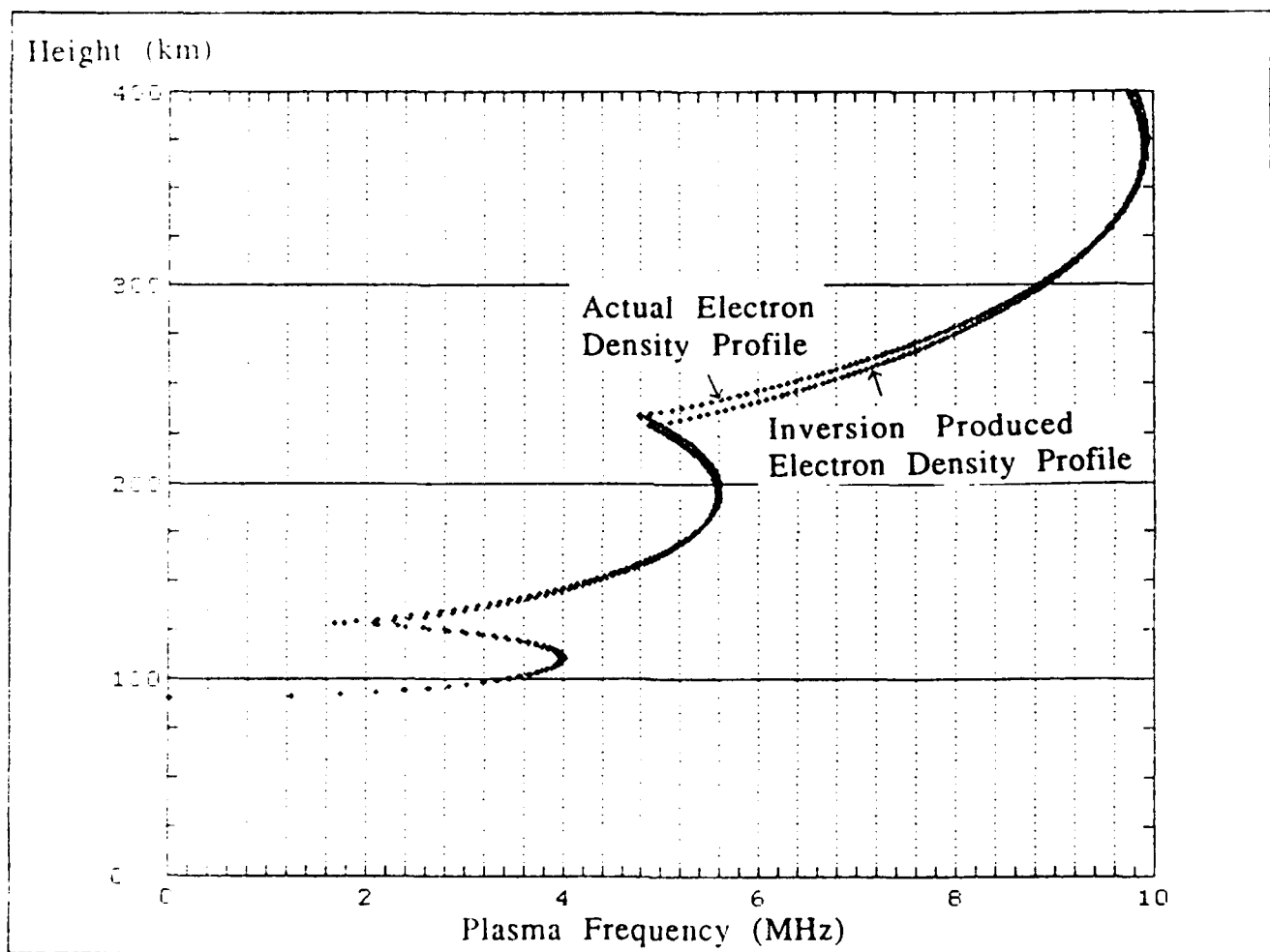
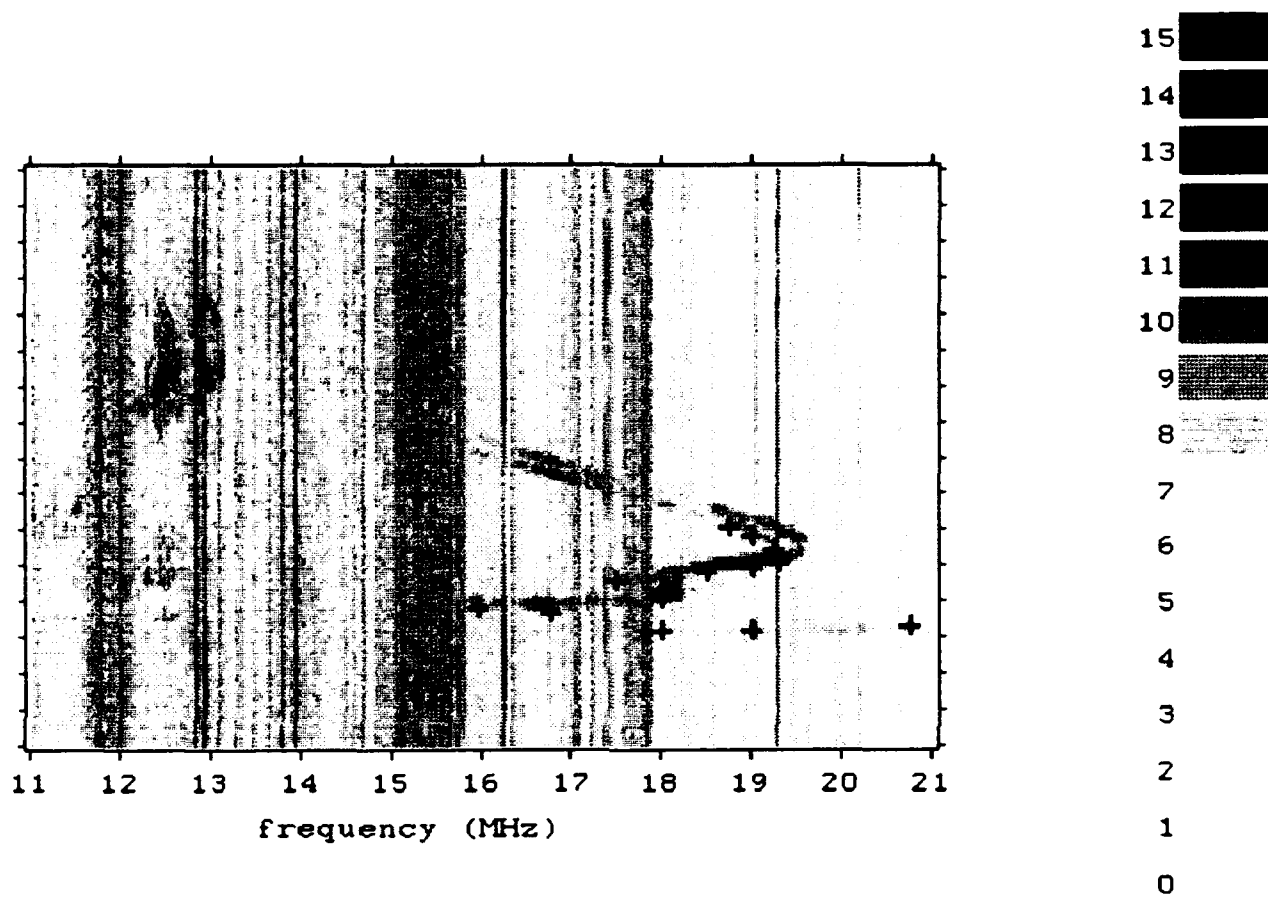


Figure 4. Inversion Using Data from Figure 3



Day 240. 18:25

Figure 5. Oblique Ionogram Goose Bay - Wallops



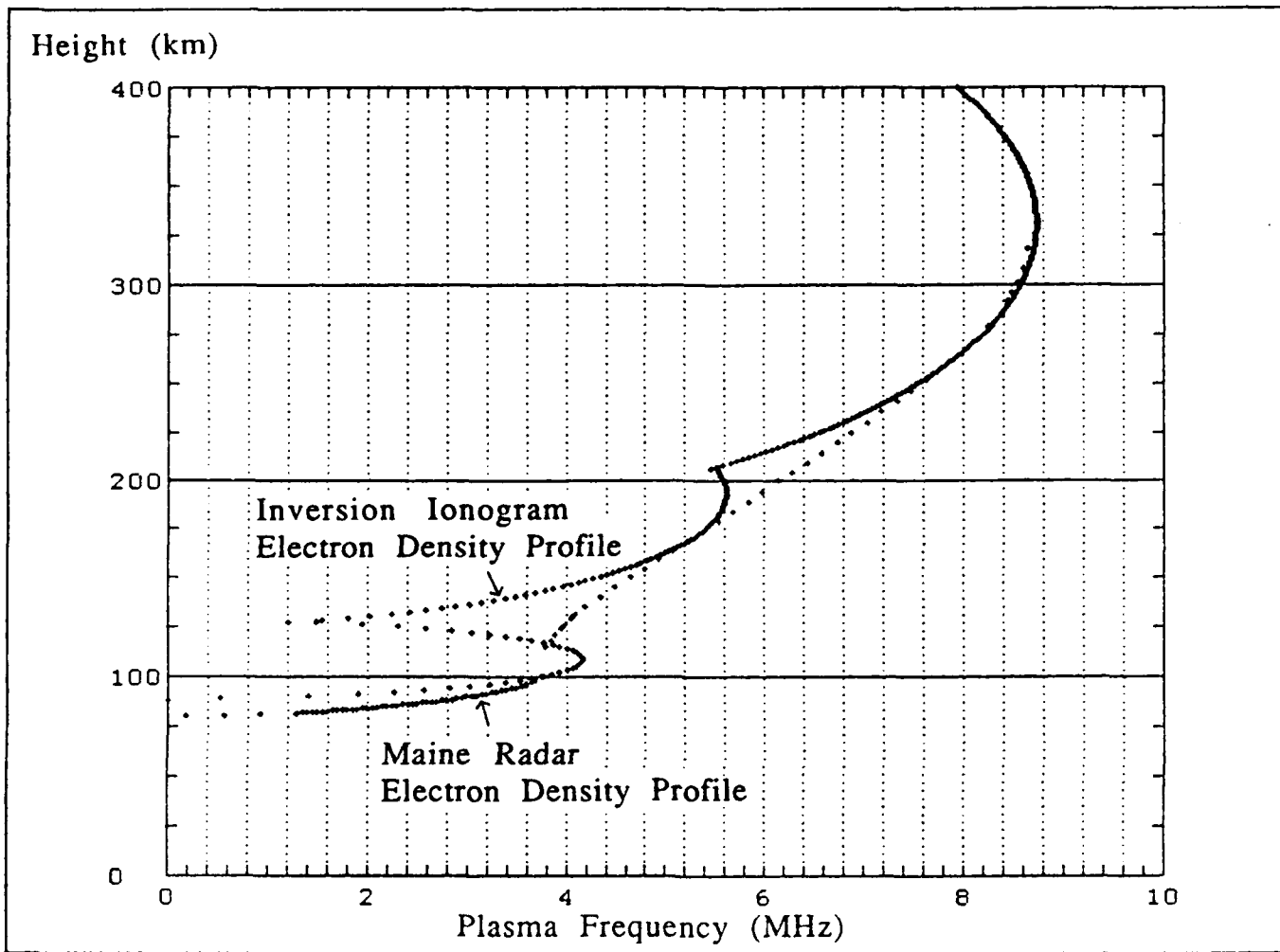


Figure 6. Inversion Using Data from Figure 5

OTH radar site. The electron density profile produced by the DORIS inversion matches the actual electron density profile quite well near and below the peaks of the F1 and F2 layers. The deep "valleys" in the DORIS profile result from the present limitation of one quasiparabolic segment per layer. The difference in the critical frequencies between the measured midpoint electron density profile and the DORIS profile occurred because no high ray E layer points were detected by the scaling algorithm. All scaled E layer points were from the region 10-20 km below the peak height. Since no constraints were placed on the E layer critical frequency, the optimization algorithm found that the best match to the observed low ray E layer group path points was obtained using a quasiparabolic layer with a critical frequency 200 KHz greater than the actual E layer critical frequency. The inclusion of a multisegment representation of each layer in an advanced version of DORIS would have corrected this type of error.

## 5.0 STATUS OF EXISTING PROCESSING SOFTWARE

The present DORIS software package that produces midpoint electron density profiles from oblique ionograms is written in Fortran. The noise suppression and trace enhancement Wiener Filter algorithm and the echo trace identification algorithm was implemented on an Apollo 3500 work station. This algorithm requires a scaled end-point vertical ionogram and noise power spectral density to process an oblique ionogram. The filtering and trace identification takes approximately 50 seconds per oblique ionogram on the Apollo platform. The inversion algorithm, also written in Fortran, was implemented in a DOS environment on a PC 386. The inversion algorithm consists of a main program and two subroutines: the first is the three layer quasiparabolic ray tracing module and the second computes the takeoff angle needed to satisfy a given group path and sounding frequency point for a specified ground range. The source code for these algorithms is available on floppy disk. Appendix B contains an operator's manual for the DORIS inversion program. The inversion software requires absolute group path vs. sounding frequency data labeled as to which echo trace they are from and whether they are high or low ray propagation modes, and a three layer quasiparabolic estimate of the midpoint electron density profile. On a 386-based PC system the current

version of the inversion algorithm takes between 2 and 8 minutes to determine the optimal midpoint electron density profile. We estimate a total DORIS run time on a 386 PC of between 4 to 10 minutes, when the autoscaling and profile inversion algorithms are combined.

## 6.0 CONCLUSION

The results of the activities conducted during the DORIS project have produced a complete prototype software package for automatic scaling and inversion of oblique ionograms. The system has been designed to utilize any available information about the desired midpoint electron density profile. Quantitative information derived from endpoint vertical ionograms and/or ionospheric models is used in the scaling and inversion. The noise cleaning and echo trace enhancement Wiener filtering method produced good estimates of the echo traces present in all of the recorded oblique ionograms. The conversion of the present off-line version of this algorithm to an on-line PC based implementation would be the only modification necessary in an operational system.

The simulated annealing optimization algorithm produces good estimates of the actual midpoint electron density profiles if at least 3 to 5 points on both the high and low rays of each echo trace are available. The time required for the present inversion algorithm to determine a midpoint electron density profile could be reduced if the annealing schedule portion of the optimization algorithm was improved. If the control parameter could be reduced at an optimal rate such that the algorithm would be better able to recognize local minima during the optimization process and produce the midpoint electron density profile faster. The general question of how to determine an optimal annealing schedule is still an active research topic and hence, the optimal annealing schedule for the oblique inversion optimization method will require additional effort.

The present echo trace scaling algorithm is the portion of the total DORIS processing program that limits overall performance. The regions of interest around each echo trace that limit the extent of the search algorithm often exclude portions of the echo trace of interest or they

contain more than one echo trace. A preliminary study of an alternative method of trace identification based on an attributed relational graph (ARG) representation of oblique ionograms has been conducted. This method, which has been proposed for other machine vision tasks, represents an oblique ionogram as a graph (Eshera and Fu, 1984). The nodes of the graph represent the primitive elements of the oblique ionogram, which in our work are a set of straight line segments. The branches of the graph represent the spatial relationships between the primitive elements. The oblique ionogram echo traces are found by first filtering the raw oblique ionogram to enhance the regions that contain potential echo trace straight line segments. The ARG representations of all possible combinations of these potential echo trace segments are compared with a reference ARG obtained from the endpoint electron density profile. The echo trace for each layer is produced from the subset of all potential echo trace segments that best matches the reference graph. The method allows both the general structure and position of each echo trace and the specific data, such as expected critical frequencies, to be used in trace identification process. The refinement and implementation of this trace identification method would produce a more robust automated oblique ionogram scaling and profile inversion algorithm.

## 7.0 REFERENCES

Eshera, M.A. and K.S. Fu, "A Graph Distance Measure of Image Analysis," IEEE Transactions on Systems, Man, and Cybernetics, SMC-14, No. 3, May/June, 1984.

Dyson, P.L. and J.A. Bennett, "A Model of the Vertical Distribution of Electron Concentration in the Ionosphere and its Application to Oblique Propagation Studies," Journal of Atmospheric and Terrestrial Physics, 50, No. 3, pp. 251-262, 1988.

Kuklinski, W.S. and J. Huth, "Application of Minimum-Mean-Square and Homomorphic Filtering Techniques to Automatic Scaling of Oblique Digital Ionograms," National Radio Science Meeting, 1987.

Kuklinski, W.S., K. Chandra and B.W. Reinisch, "Status of DORIS Automatic Scaling," GI-TR-89-0184, Scientific Report No. 13, October 1988.

Kuklinski, W.S., K. Chandra and B.W. Reinisch, "Progress of DORIS Automatic Scaling," GL-TR-89-0186, Scientific Report No. 15, January 1989.

Kuklinski, W.S., K. Chandra and B.W. Reinisch, "Automation of Oblique Propagation Measurements, Oblique Trace Identification and Inversion," GL-TR-90-0089, Scientific Report No. 22, January 1990.

Kuklinski, W.S., B.W. Reinisch, G.S. Sales and J. Buchau, "From Oblique Ionograms to Mid-Point Electron Density Profiles," 1992 National Radio Science Meeting, 1992.

Reinisch, B.W., K. Bibl, D.F. Kitrosser, G.S. Sales, J.S. Tang, Z.M. Zhang, T.W. Bullett and J.A. Ralls, "The Digisonde 256 Ionospheric Sounder," World Ionosphere/Thermosphere Study, WITS Handbook, Vol. 2, Ed. by C.H. Liu, December 1989.

Reinisch, B.W., D.M. Haines and W.S. Kuklinski, "The New Portable Digisonde for Vertical and Oblique Sounding," AGARD Proceedings Number 502, pp. 11-1 to 11-11, 1991.

## **APPENDIX A**

**The New Portable Digisonde for Vertical and Oblique Sounding**

**AGARD Conference Proceedings 502  
Remote Sensing of the Propagation Environment  
Cesme, Turkey  
October 1991**

---

# AGARD

ADVISORY GROUP FOR AEROSPACE RESEARCH & DEVELOPMENT

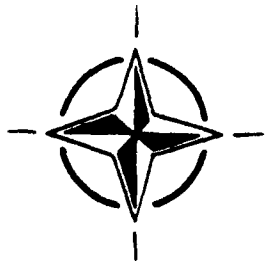
7 RUE ANCELLE 92200 NEUILLY SUR SEINE FRANCE

---

**Paper Reprinted from  
AGARD Conference Proceedings 502**

## **Remote Sensing of the Propagation Environment**

(La Télédétection du Milieu de Propagation)



**NORTH ATLANTIC TREATY ORGANIZATION**

THE NEW PORTABLE DIGISONDE  
FOR  
VERTICAL AND OBLIQUE SOUNDING

Bodo W. Reinisch  
D. Mark Haines  
Walter S. Kuklinski  
University of Massachusetts Lowell  
Center for Atmospheric Research  
450 Aiken Street  
Lowell, MA 01854  
USA

## SUMMARY

A small low cost digital ionosonde, the Digisonde Portable Sounder (DPS) has been developed which uses 500 $\mu$ s, 10% duty factor, wide pulses for vertical sounding and 8.5ms pulses for oblique sounding. Intrapulse coding and pulse compression techniques result in a 67 $\mu$ s resolution for both waveforms. A new autoscaling technique for oblique ionograms inverts the oblique echo traces into midpoint electron density profiles that are modeled as a sum of quasiparabolic layers.

## 1. INTRODUCTION

Reliable high frequency (HF) communication, Over-the-Horizon radar tracking, and HF direction finding all depend on good real time knowledge of the ionosphere. In the last decade modern digital ionosondes (Reinisch, 1986) became available that automatically analyze the vertical ionograms and provide, in real time, the vertical electron density profiles for the location of the sounder (Reinisch et al., 1990). For many HF applications the ionosphere must be specified in a large area and a network of ionosondes is required. The new Digisonde Portable Sounder (DPS) has been designed for optimal efficiency in such a network by providing the necessary hardware and software for both vertical and oblique (bistatic between DPS stations) sounding.

For vertical sounding the transmitter pulse width is limited to about 500 $\mu$ s considering the pulse propagation time of 600 $\mu$ s for E region echoes. Intrapulse phase coding and pulse compression techniques provide a range resolution of 67 $\mu$ s (or 10 km). For quasi-vertical or bistatic sounding the DPS transmits 8.5ms pulses at 100% duty cycle with the same range resolution of 67 $\mu$ s. A DPS network can accurately map the ionosphere if both vertical and oblique ionograms are used to specify the electron density profiles at the locations of the sounders as well as at their mid-points. Any successful IIF

application requires "now-casting" for the ionospheric propagation medium, i. e. current specification of the ionospheric region used by the HF link. Automatic scaling of the vertical and oblique ionograms in real time provides the inputs for the now-casting.

Autoscaling of the vertical ionograms is achieved with the ARTIST software (Reinisch and Huang, 1983, Gamache et al., 1985) which is routinely used in some forty Digisonde 256 sounders worldwide (Reinisch et al., 1990). New autoscaling for oblique ionograms and inversion to midpoint quasiparabolic electron density profiles is described in Section 3 of this paper. Section 2 gives a brief description of the Digisonde Portable Sounder.

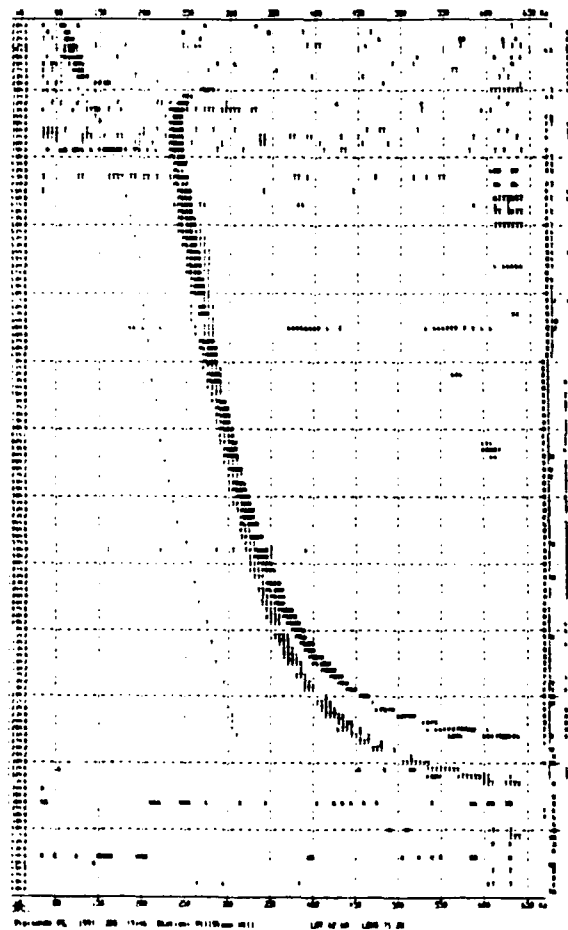
## 2. DESCRIPTION OF THE DIGISONDE PORTABLE SOUNDER

Ground based HF observations of the ionosphere rely on the accurate measurement of the following observables:

1. frequency
2. height/range (time delay)
3. amplitude
4. phase
5. Doppler shift or spread (frequency dispersion)
6. wave polarization (left or right hand)
7. angle of arrival

All of these parameters are measured simultaneously by the DPS and as many as five are displayed at once in the various display modes available. For instance, the Doppler Ionogram in Figure 1 (Millstone Hill, 4 November 1991) represents an echo at a given frequency and height by its position in the display. The amplitude (in 2dB) is represented numerically by an optically weighted font, the Doppler shift is represented by shades of color while the polarization is represented by the color group. This paper shows a black/white printout using the letter X to indicate X-echoes. The





automatically scaled leading edges of the E and F-traces are identified by the letters E and F, and the electron density profile is indicated by the letter T.

Gaussian noise distribution which is actually a best case), measuring Doppler spectra to 1% amplitude accuracy requires over 20dB SNR, and precision ranging by the  $df/dt$  technique requires better than 20dB SNR. Making a small inexpensive portable sounder requires use of a small low power transmitter which makes it difficult to achieve the required SNR. However, advanced digital signal processing techniques in the DPS overcome this difficulty.

The DPS (Fig. 2) is a software implementation of the well proven measurement techniques used by the Digisonde 256 sounder (Reinisch et al. 1989) developed some ten years ago at the University of Lowell Center for Atmospheric Research (ULCAR). Pulse compression techniques allow reduction of the transmitter peak pulse power from 10kWatt (for the Digisonde 256) to 500Watt.

## Signal Processing

As mentioned above, the requirement for a good SNR seems incompatible with a small, lightweight, low-cost portable system, however by lengthening the transmitted pulse of a small low voltage solid state transmitter we can transmit an amount of energy per pulse equal to that transmitted by a high power pulse transmitter without having to provide components to handle the large voltages. The range resolution is recovered by phase modulation using an optimized phase code. This intrapulse modulation allows pulse compression in the receiver to restore a 10km resolution to separate the echoes from different ionospheric layers. The compressed pulse must, to an acceptable degree, reproduce a simple rectangular pulse (i.e. the spurious output of the pulse compression process must not obscure other signals of interest) and for monostatic operation (colocated transmitter and receiver) the entire waveform must be transmitted before the first echo of interest is received. Therefore, for vertical incidence sounding we selected an 8

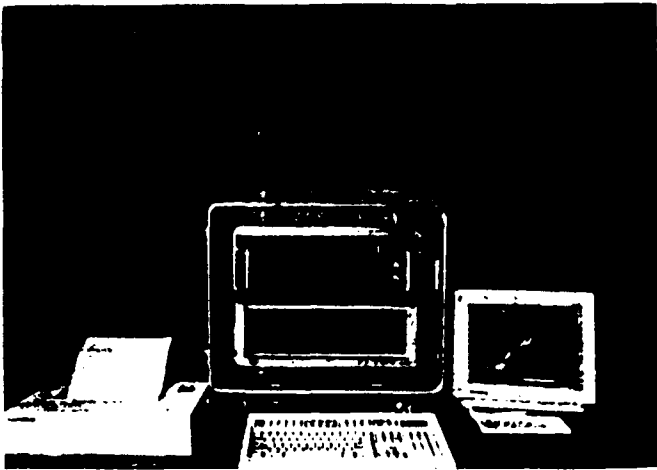


Figure 2a. Digisonde Portable Sounder

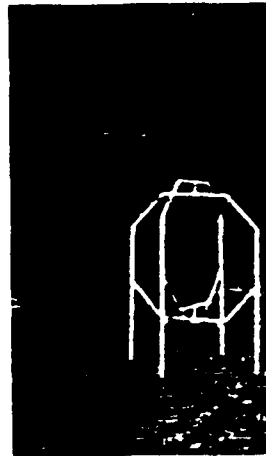


Figure 2b. Turnstyle Antenna

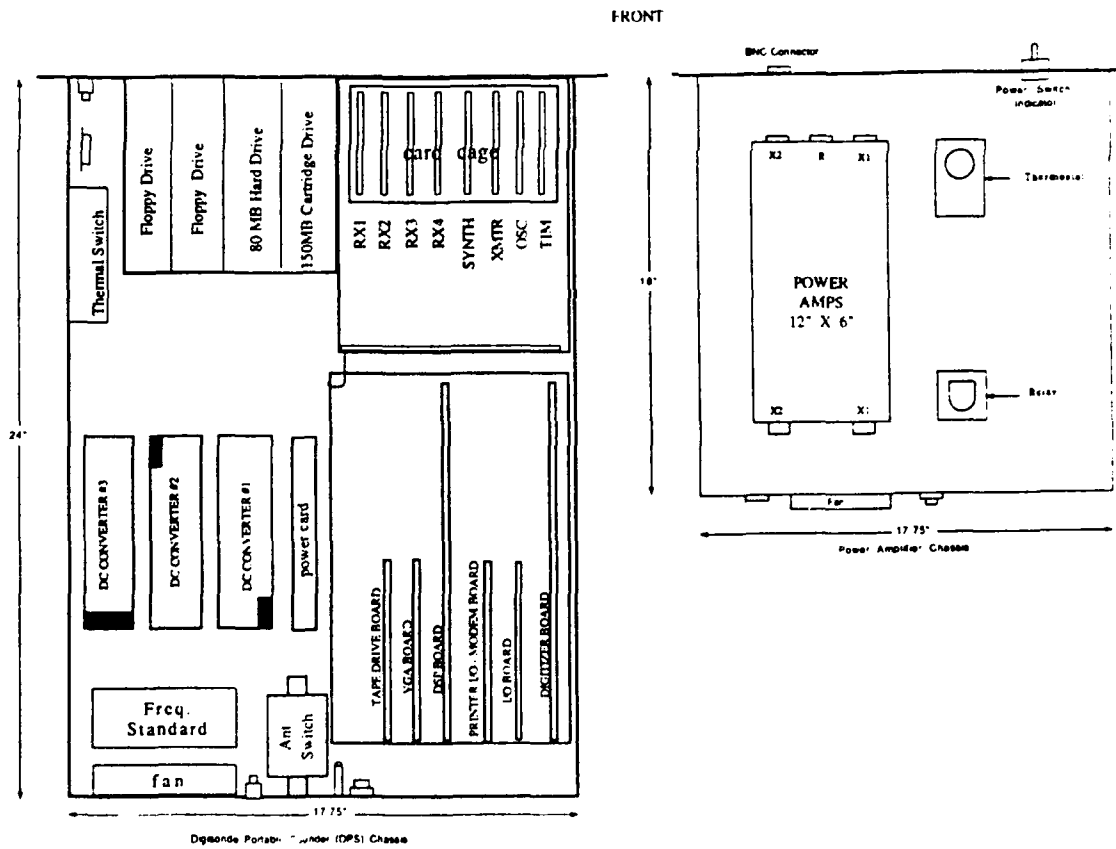


Figure 3. DPS Chassis Configuration

bit complementary (Golay, 1961) phase code pair modulated onto a 533 $\mu$ sec pulse which provides 12dB of SNR improvement upon pulse compression.

For bistatic operation such as oblique sounding or backscatter sounding, a 100% duty cycle CW (continuous wave) waveform can be used since the transmission need not be extinguished prior to sampling data at the receiver. For this mode of operation we have selected the 127 bit maximal length sequence code (Sarwate and Pursley, 1980) which allows pulse compression with a 21dB signal-to-noise ratio improvement while only producing 0.9% spurious amplitude response at ranges (time delays) other than the true range.

Added to the 12 or 21dB of pulse compression gain is the SNR gain offered by the Doppler integration process (also used in the Digisonde 256) which for 128 line Doppler spectra is 21dB. The effect of all this signal processing is tremendous. For instance, compared to the 500Watt DPS oblique waveform with its 42dB SNR improvement, a single pulse, non-integrating measurement system would require 8MWatts of transmitter power to obtain an equivalent SNR. Even a somewhat sophisticated system which coherently integrates 8 pulses (any more than 8 would require "Digisonde-like" Doppler processing due to Doppler induced phase changes over the integration period), would require a 1MWatt transmitter in order to be equivalent.

### Multiplexing

Using any of the above waveforms, the Digisonde Portable Sounder allows multiplexed Doppler integration of up to 64 separate combinations of frequencies, antennas (the system includes 4 phase matched receiving antennas), and polarizations (i.e. ordinary or extraordinary propagation modes, hereafter referred to as O and X). This multiplexing is implemented by changing the system's operating parameters from pulse-to-pulse. This essentially simultaneous measurement at multiple frequencies, antennas and polarizations is accomplished by synchronizing the computer's data acquisition and signal processing software to the transmitted waveform through a hardware interrupt. The interrupt is timed to occur just 250 $\mu$ sec prior to the occurrence of a transmitted pulse, or coded waveform, such that the frequency, antenna selection, gain, polarization, or waveform can be changed in a pre-computed sequence. The switching of any or all of these parameters is accomplished in 22 $\mu$ sec giving the system ample time (about 200 $\mu$ sec) to settle before transmitting. At the end of the

multiplexed Doppler integration the system contains an entire Doppler spectrum for each resolvable range, each receive antenna, each frequency and each polarization measured, up to 8192 128-line complex spectra. The real-time pulse compression and Doppler processing is performed in a digital signal processor embedded within the system which is fast enough to allow it to keep up in real-time with the data acquisition. The pulse-to-pulse control offers the flexibility to optimize the multiplexing process for any of a number of different types of measurements. A few of these are:

1. Angle of arrival. Since the data on four spaced receiving antennas is acquired quasi-simultaneously, the signal phases measured on each of the antennas can be used to compute an angle of arrival for each range and Doppler component of the received signal.
2. Precise Group Height. By observing the change in phase of a signal as a function of small changes in frequency (e.g. 10kHz), the altitude of a reflecting layer can be determined with high accuracy. The limitation is signal-to-noise ratio dependent, but accuracies of 100's of meters are routinely achievable. The time history of the precise height can be measured by repeated soundings at a fixed frequency.
3. Identification of O or X Propagation Mode. By simultaneously integrating all heights at both polarizations, the detected echo is compared in the two separate data buffers to determine which receive polarization produced a larger response, therefore even elliptically polarized signals can be declared O or X even though some of the echo amplitude "leaks" into the wrong polarization channel.
4. High Doppler Resolution. Although high Doppler resolution could be achieved simply by slowing down the pulse repetition rate or producing extremely large Doppler spectra (e.g. 4096 complex Doppler lines), both approaches increase the time required to make measurements. Since the ionosphere rarely produces more than a few Hertz of Doppler shift the Doppler analysis of pulses transmitted at a 200Hz rate (giving a Doppler range of  $\pm 100$ Hz) is usually inefficient. However, by simultaneously integrating 16 sounding frequencies, the Doppler range is brought down to  $\pm 6$ Hz, which can provide 0.094Hz Doppler resolution rather than 1.5Hz. At the end of this multiplexed integration 16 frequency steps have been measured and are ready for display. This high Doppler resolution swept frequency ionogram is performed

16 times faster than would be possible with a conventional non-multiplexed mode of operation.

### Automatic Sequencing

An operator who is only casually familiar with the inner workings of a DPS sounder can easily compose some very complex measurement sequences by selecting programmed measurement parameters from an interactive screen. The parameters presented on the screen specify frequency range, frequency resolution, multiplexing parameters, height resolution, Doppler range and resolution, data storage formats and automatically schedule unmanned operation. Since there are up to 8,192 Doppler spectra in memory at the end of a coherent integration, and typically less than 1% is useful data at the end of a coherent integration, data storage formats allow the user to specify criteria for reducing the amount of data stored:

- a. selection of 1 maximum amplitude in each Doppler spectrum per height measured.
- b. storage of spectra from of a limited number of heights around the leading edge of a layer.
- c. storage of a limited number of Doppler lines around zero for each height measured.
- d. or storage of everything available (i.e., a scattering function which is all Doppler lines at all ranges measured).

The program and schedule settings selected by the user (either remotely or locally) during an interactive editing session are stored in a hard disk file and become the new default settings the next time the system is turned on.

### Oblique Sounding

Before addressing the use of oblique sounding data for the characterization of the ionosphere at the midpoint, we will describe this operating mode. In addition to the CW waveform, the DPS has optimized oblique channel measurements by providing precision timing, a highly stable frequency source and automatic synchronization with distant transmitters. All timing waveforms are generated from a counter chain which can be driven by a Rubidium frequency standard. The counter chain can be synchronized to an "external" 1 PPS (pulse per second) timing reference (typically GPS, GOES satellite clock, or LORAN) and will maintain synchronization to 1μsec accuracy. The internal timing signals can be offset by a pre-determined amount (i.e. a menu parameter) up to 0.5 seconds to compensate for propagation time delays. Therefore, each transmitted pulse occurs just as the receiving system expects it.

The oblique ionogram data stored for midpoint measurements is a 16 line Doppler spectrum at each of 256 heights (time delays) providing 96 dB of dynamic range in 0.375dB steps. This data is stored on a disk file and on a tape cartridge and the midpoint profile processing can proceed.

## **3. ADAPTIVE OBLIQUE IONOGRAM SCALING AND PROFILE INVERSION**

We have developed an adaptive set of robust algorithms to automatically scale and invert oblique ionograms. These algorithms utilize one or both scaled end point vertical ionograms to estimate the oblique ionogram. This estimate, which is used by subsequent filtering and trace identification algorithms, is updated whenever the vertical ionograms change.

### Algorithm Development

The automatic oblique ionogram scaling algorithm uses a tracking algorithm (Sun, 1989) to determine the leading edge points of each echo trace. These scaled leading edge points are used directly to calculate a midpoint electron density. The direct inversion process, assumes each ionospheric layer can be modeled with a quasi-parabolic electron density profile. This inversion technique requires the absolute group path information that is provided by the synchronized operation of two Digisondes. The tracking algorithm uses the scaled vertical ionogram, produced in the end point Digisonde, to synthesize the echo traces that would be measured over the oblique link if the midpoint ionosphere and the ionosphere at the transmitter were identical. While the overhead and midpoint ionospheres are typically not equal, they are similar enough to provide an excellent starting point from which any differences between the ionosphere at these two locations can be determined. These synthesized oblique echo traces are also used in a noise suppression filter and subsequent trace identification algorithm. The utilization of these real-time synthesized oblique echo traces produces an adaptive algorithm whose performance is superior to a non-adaptive approach.

### Frequency Redundancy Filter

The first operation performed on the received oblique ionogram is a frequency redundancy noise suppression. A 100kHz oblique ionogram, which has sufficient resolution for calculating the equivalent midpoint electron density profile, is generated from either 25 or 50kHz sounding data by selecting the highest signal-to-noise ratio channel from each set of four adjacent 25 kHz soundings or two adjacent 50kHz soundings.

### Noise Suppression Wiener Filter

The subsequent noise suppression filter uses an adaptive minimum-mean-square Wiener filtering technique (Andrews and Hunt, 1969, Kuklinski et al., 1990). The 100kHz oblique ionogram is modeled as the sum of a noise/interference signal and the desired noise free oblique autotraces. The Wiener filter is produced by dividing the power spectral density of the synthesized oblique echo traces by the sum of the power spectral densities of the synthesized oblique echo traces and an estimate of the noise power spectral density as shown in equation (1).

$$H(\omega_t, \omega_f) = \frac{P_{et}(\omega_t, \omega_f)}{P_{et}(\omega_t, \omega_f) + P_n(\omega_t, \omega_f)} \quad (1)$$

The noise power spectral density was calculated from ionograms recorded while the transmitter was off, using a two-dimensional periodogram technique. Typical results are shown in Figure 4. The upper panel is a representative 100kHz oblique ionogram with the corresponding filtered ionogram in the lower panel.

The synthesized oblique echo traces, derived from the end point ionograms, are also used to define regions of interest for subsequent processing. These regions of interest, as shown in the upper panel of Figure 5, are defined as all points within a specified number of group path range bins and sounding frequencies of the synthesized oblique echo traces. At present the allowable variations were derived from the variances of an oblique ionogram data base. Any echoes in the region of interest for a particular layer is considered to be part of the echo trace for that layer.

The tracking algorithm determines, at a given sounding frequency, where the echo trace most closely matches an assumed template of echo trace amplitudes. To obtain this optimal location, the template is translated and rotated about an initial estimate. The mean square difference between the actual echo trace amplitudes and the template is used by two sequential gradient searches, one for translation and one for rotation, to determine the optimal location. The results of this local search process are the locations of the center, leading and trailing edges of the echo trace. The algorithm uses this information to estimate the group path of the echo trace at the next sounding frequency to be processed. The template matching procedure is repeated until the entire echo trace is scaled in this manner.

### Midpoint Profile Modeling

Our technique assumes that the ionosphere at the midpoint can be modeled by one or more quasiparabolic (QP) segments (Dyson and Bennett, 1988). In principle, the parameters that define a single QP layer can be calculated from any three pairs of group path vs. sounding frequency data since the ground range between transmitter and receiver is known. In practice however, the numerical sensitivity of the equations that relate the group path and ground range of a ray to the take-off angle and QP layer parameters, causes these three point solutions to be unstable. The tracking algorithm utilized here has the flexibility to produce the required number of scaled leading points for a numerically stable inversion.

The inversion algorithm uses a simulated annealing optimization method to determine the QP electron density profile (Croft and Hoogasian, 1968) for each layer. The QP layer is defined as :

$$N_e = \begin{cases} N_m \left[ 1 - \left( \frac{r-r_m}{y_m} \right)^2 \left( \frac{r_b}{r} \right)^2 \right] & r_b < r < r_m \left( \frac{r_b}{r_b - y_m} \right) \\ 0 & \text{elsewhere} \end{cases}$$

where  $N_e$  = electron density,  $r$  = radial distance from earth center,  $r_b$  = radial distance to the bottom of the layer,  $r_m$  = radial distance of maximum electron density,  $N_m$  = maximum electron density, and  $y_m$  the layer semithickness.

The E layer QP parameters are determined from the scaled oblique E echo points. This QP E layer and the scaled oblique F1 echo points are used to determine the F1 layer QP parameters and, if an F2 trace is present, the E and F1 layer QP parameters and the scaled oblique F2 echo points are used to determine the F2 layer QP parameters.

The multilayer QP model produces the following analytical relationships for the group path,  $P'$ , and the ground range,  $D$ , of a ray in terms of takeoff angle, sounding frequency, and layer parameters.

$$D = \sum g_{1i}(r_{mi}, y_{mi}, N_{mi}, \beta, f) \quad (2)$$

$$P' = \sum g_{2i}(r_{mi}, y_{mi}, N_{mi}, \beta, f) \quad (3)$$

where  $i$  is the layer index,  $\beta$  is the ray takeoff angle, and  $f$  is the sounding frequency.

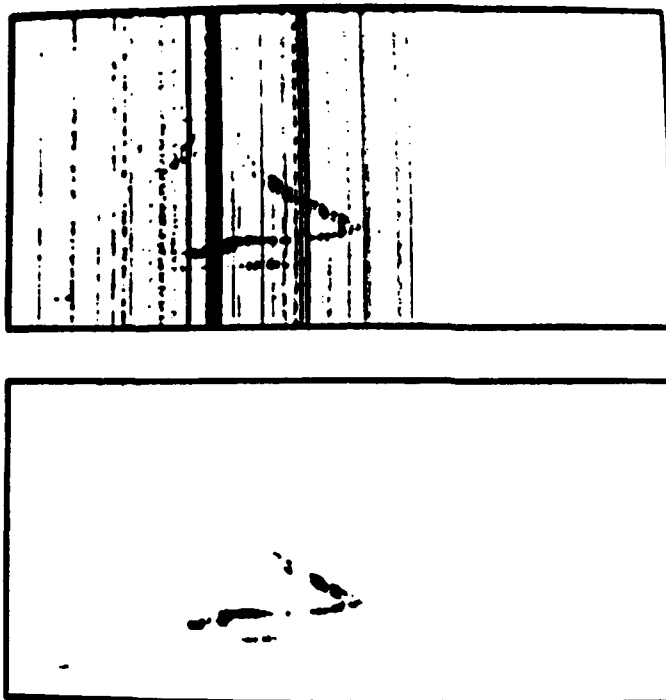


Figure 4. 100kHz Oblique Ionogram Produced via the Frequency Redundancy Technique (Upper). Resulting 100kHz Oblique Ionogram After Processing through the Modified Wiener Trace Enhancement Algorithm and the Noise Suppression Technique (Lower). Goose Bay, Labrador to Millstone Hill, Massachusetts; April 5, 1988, 1908 UT.

Year : 88 Day : 096 Time : 18:59:05

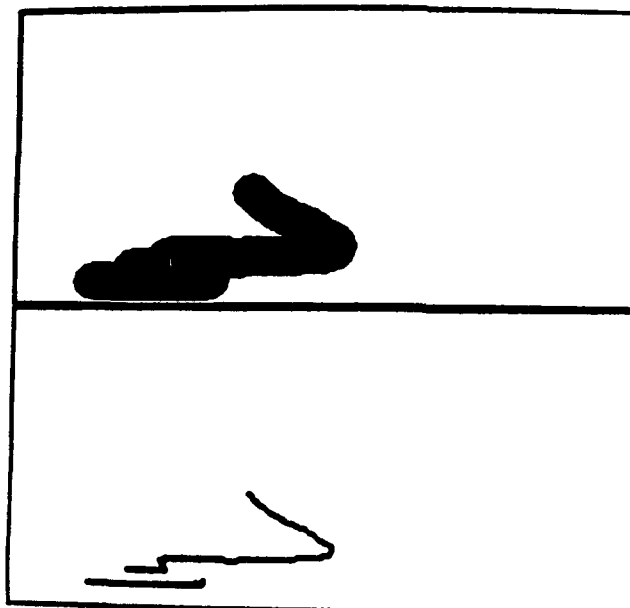


Figure 5. End Point Synthesized Oblique Ionogram via Secant Law (Lower). Region of Interest Calculated from the E and F Layers of the Corresponding Vertical Ionogram (Upper). Goose Bay, Labrador to Millstone Hill, Massachusetts; April 5, 1988, 1859 UT.

The simulated annealing optimization technique we use to determine the QP electron density profile has been applied to solve many large scale combinational optimization problems (van Laarhoven and Aarts, 1988). In these optimization problems an objective function that depends on the configuration of a large set of system parameters is minimized. In the QP electron density profile inversion problem, the system is the collection of quasiparabolic segments used to model the midpoint ionosphere. The objective function used in the electron density inversion is the sum of the squared differences between the group paths calculated from the QP model and those obtained from the scaled oblique ionograms.

Typical results are seen in Figures 6, 7 and 8. The left panels of each figure show the group paths calculated from the QP electron density model (dots) in relation to the oblique ionogram. The right panels are the corresponding ground ranges in relation to the known ground range (straight line). Seven scaled points from the oblique ionogram were used in this example. The upper panels of Figure 6 contain the original scaled oblique ionogram and the known ground range. The middle panel of Figure 6 shows the group paths and ground ranges of the seven rays for the initial estimates of the layer parameters and rays takeoff angles. Any group path differences greater than 500km are plotted as being equal to 500km, hence the four group path points at the top of the left middle panel of this figure. After the first iteration the three low angle ray group paths are within 41km of the actual oblique data, while the three low angle ray ground ranges are within 43km of the actual ground range. Figure 7 contains the data obtained for iterations 3 through 5 in the upper, middle and lower panels respectively, while Figure 8 contains the corresponding data for iterations 6 through 8. As the iterations are performed the algorithm converges to a QP layer that minimizes the total difference between the measured and calculated oblique ionograms. By the eighth iteration (lower panel of Figure 8) the largest group path difference between the actual data and the quasiparabolic model is 4km, while the largest ground range difference is 6km.

#### 4. CONCLUSION

A small low cost ionospheric sounder has been developed and tested that is optimally suited for automated vertical and oblique sounding. Automatic scaling algorithms for the vertical as well as the oblique ionograms provide the vertical electron density profiles at the sounder locations and at the midpoints. While the real time

scaling profile inversion of the vertical ionograms has become a routinely applied technique, the automatic scaling of oblique ionograms in terms of quasiparabolic midpoint profiles is still at an experimental stage.

#### Acknowledgement

This research was in part (autoscaling of oblique ionograms) supported by Air Force Contract No. F19628-90-K-0029 under the "DORIS" subline item.

#### 5. REFERENCES

- Andrews H. C. and Hunt B.R., "Digital Image Processing," Prentice-Hall Co., 1969.
- Croft T. A and Hoogasian H., "Exact Ray Calculations in a Quasiparabolic Ionosphere With No Magnetic Field," Radio Science, 3, p 69., 1968.
- Dyson, P.L. and Bennett, J.A., "A Model of the Vertical Distribution of the Electron Concentration in the Ionosphere and its Application to Oblique Propagation Studies," Journal of Atmos. and Terr. Phys., 50, 3, pp. 251, 1988.
- Gamache, R.R., Kersey, W.T., and Reinisch, B.W., "Electron Density Profiles from Automatically Scaled Digital Ionograms. The ARTIST's Valley Solution," Scientific Report No. 1, AFGL-TR-85-0181, ULRF-434/CAR, Air Force Geophysics Laboratory, 1985.
- Golay, M.J., "Complementary Codes," IRE Transactions on Information Theory, April, 1961.
- Kuklinski W. S., Kitrosser D. F., Reinisch B.W., "Automation of Oblique Propagation Measurements Oblique Trace Identification and Inversion," Scientific Report, No. 22, GL-TR-90-0089, ULRF-465/CAR, Air Force Geophysics Laboratory, January 1990.
- Laarhoven van, P.J.M. and Aarts E.H.L., "Simulated Annealing Theory and Applications," D. Reidel Publishing, 1988.
- Reinisch, B.W. and Huang, X., "Automatic Calculation of Electron Density Profiles from Digital Ionograms, 3, Processing of Bottomside Ionograms," Radio Science, 18, 477, 1983.
- Reinisch, B.W., Bibl, K., Kitrosser, D.F., Sales, G.S., Tang, J.S., Zhang, Z.M., Bullett, T.W., and Ralls, J.A., "The Digisonde 256 Ionospheric Sounder," World Ionosphere/Thermosphere Study, WITS Handbook, Vol. 2, Ed. by C.H. Liu, December 1989.

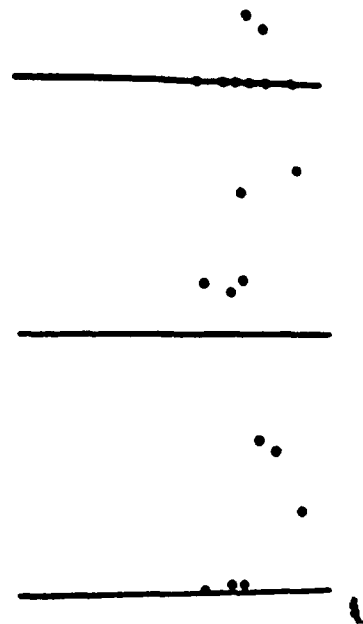
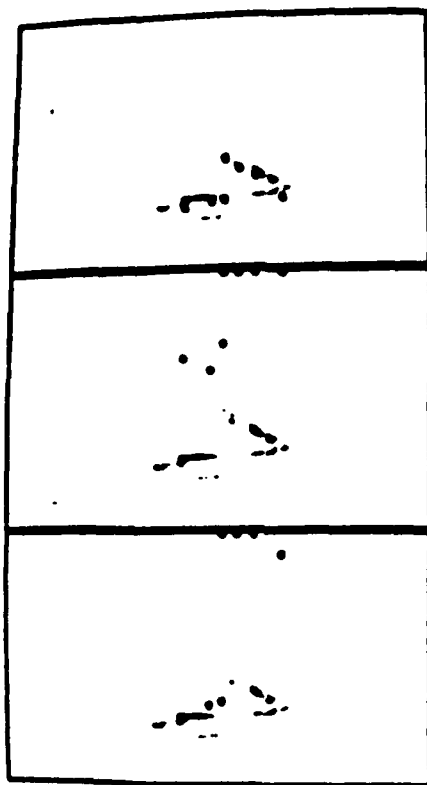


Figure 6. Algorithm Convergence Properties, Iterations 0 through 2.

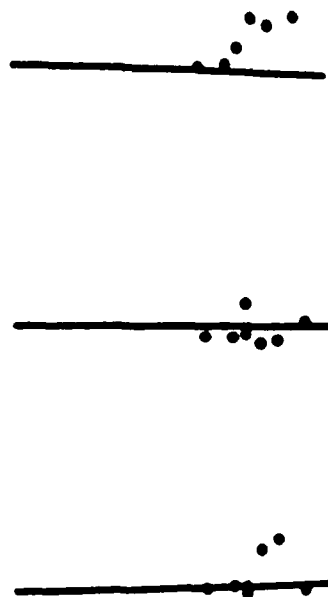
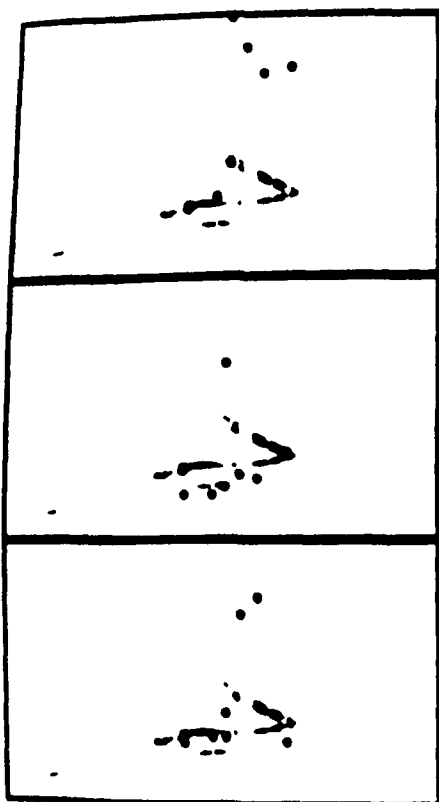


Figure 7. Algorithm Convergence Properties, Iterations 3 through 5.



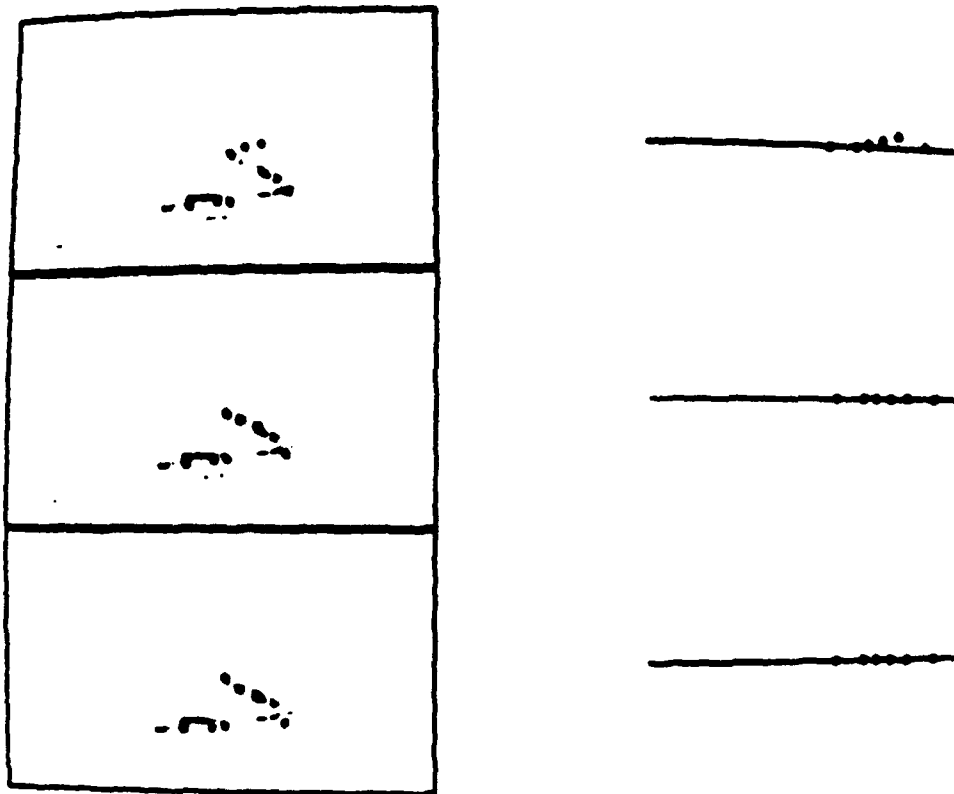


Figure 8. Algorithm Convergence Properties, Iterations 5 through 7.

Reinisch, B.W., Gamache, R.R. and Bossy, L.G., "Ionospheric Characteristics for IRI in Real Time," *Adv. Space Res.*, 10, 8, pp. (8)25-(8)34, 1990.

Reinisch, B.W., "New Techniques in Ground-Based Ionospheric Sounding and Studies," *Radio Science*, 21, 3, pp. 331-341, May-June 1986.

Sarwate, D.V. and Pursley, M.B., "Crosscorrelation Properties of Pseudorandom and Related Sequences," *Proceedings of the IEEE*, 68, 5, May, 1961.

Sun Y., "Development of a Coronary Artery Blood Vessel Tracking Algorithm," *IEEE Transactions on Medical Imaging*, 8, 1, p78, 1989.

## DISCUSSION

### **C. GOUTELARD**

Votre communication est très intéressante et elle m'a passionné au point de vous poser deux questions.

Vous signalez que la puissance équivalente en impulsion de votre système est de 8MW. Il me semble cependant que vous effectuez un traitement post-correlation par transformée de Fourier. Il faudrait tenir compte d'un traitement similaire dans le cas du système impulsionnel. De plus en télédétection où la fonction d'ambiguïté du signal doit être prise en compte les codes continus se trouvent pénalisés. Pouvez-vous faire un commentaire?

Ma deuxième question porte sur le modèle que vous utilisez pour l'ionosphère, un modèle à trois couches quasi paraboliques. Cela permet de mener des calculs analytiques. Nous utilisons un modèle proche de celui de Bradley Dudeney avec 2 couches quasi paraboliques et 1 couche quasi linéaire. Nous menons comme vous des calculs analytiques - par exemple avec des équations de Lagrange - pour modéliser la propagation. Quel est votre avis sur l'opportunité d'utiliser l'un des modèles plutôt que l'autre?

*Your paper is very interesting and it impressed me so much that I should like to ask you two questions:*

*You state that the equivalent pulse power of your system is 8MW. It seems to me however, that you carry out post-correlation processing using a Fourier transform. Similar processing would need to be allowed for in the pulsed system. What is more, the continuous codes are penalised in remote sensing, where allowance needs to be made for the ambiguity function of the signal. Would you care to comment ?*

*My second question concerns the model which you use for the ionosphere, a model with three quasi parabolic layers. This enables one to make analytical calculations. We use a model similar to the one produced by Bradley Dudeney with 2 quasi parabolic layers and 1 quasi linear layer. Like you, we make analytical calculations - using Lagrange equations for example - to model propagation. What do you think is the advisability of using one model rather than the other ?*

### **AUTHOR'S REPLY**

1. For oblique sounding we use the 127 bit maximal length sequence code providing 21 dB S/N improvement. Another 21 dB S/N gain is obtained by the 128 point Doppler integration. 42 dB over 500 W corresponds to 8 MW of a single pulse no-integration system. Without spectral integration (like in the Digisonde) one should not phase-coherently integrate more than 8 pulses (to avoid loss of Doppler shifted echoes). This requires 1 MW for the same S/N ratio.
2. The Bradley-Dudeney profile may have an advantage over the 3 parabola model in that it has less harsh discontinuities between the layers. We prefer the parabolic model since it can be made completely smooth (continuous first derivative) by adding two inverted parabolas between the layer parabolas. Fast analytical ray tracing through parabolic sections of the ionosphere exists. Stability of the inversion solutions is good for our technique, I do not know what it would be for the B-D profile.

### **E. SCHWEICHER**

1. Did you use a Barker code or some other pseudo-stochastic code?
2. Did you perform your pulse compression by software or by hardware?

### **AUTHOR'S REPLY**

1. A complementary 8 bit code is used for vertical sounding in a "moderate" ionosphere. The Barker code is used in a high-Doppler (polar cap) ionosphere.
2. Software pulse compression.

(THIS PAGE LEFT INTENTIONALLY BLANK)

## **APPENDIX B**

### **Operator's Manual for DORIS Profile Inversion**

UNIVERSITY OF MASSACHUSETTS LOWELL  
CENTER FOR ATMOSPHERIC RESEARCH

450 Aiken Street  
Lowell, MA 01854

OPERATOR'S MANUAL FOR DORIS PROFILE INVERSION

April 1992

Running the DORIS profile inversion software requires, as a minimum, the following PC system:

Central Processing Unit:	Intel 80386 or higher
Math Co-Processor:	Intel 80387 or higher
Memory Size:	640 kb or larger
Hard Disk with at least 4 free Mb	
Video Adapter:	Color Graphics with VGA Mode
Monitor:	NEC Multisync
or equivalent	
Operating System:	DOS 3.0 or higher

The ULCAR supplied ADEP (ARTIST Data Editing and Printing) system fulfills this requirement.

To use the off-line DORIS SOFTWARE, do the following:

Go to the DORIS directory on the 'C' drive by typing after the prompt:

```
C:\ <CR>  
CD DORIS.
```

At this point, if you type DIR, you will get a listing of all the files in this DIRECTORY. The executable files have the extension .EXE. There are 3 executable files: GENSYN.EXE, OBL\_INVR.EXE and PLOTSYN.EXE.

The OBL\_INVR program produces mid-point electron density profiles from scaled oblique ionograms. To run this program type after the prompt:

```
OBL_INVR
```

then you will be prompted to input the scaled trace data file. A sample of this file is named SCLDATA. Type SCLDATA.

The inversion algorithm requires at least 2 scaled points for each mode (high ray and low ray) of each layer E, F1, F2, resulting in 12 as the

modes/layer) (3 layers). The first line of this file is the number of scaled points. The subsequent lines are the scaled points. The first column is the sounding frequency. The second column is the absolute group path. The third column is either:

- 1 for low ray E
- 1 for high ray E
- 2 for low ray F1
- 2 for high ray F1
- 3 for low ray F2
- 3 for high ray F2

A listing of this file is enclosed.

The program will then prompt you for the output file name. Type after the prompt the file name. Type (in this case the output is demo 1) DEMO 1.

Then enter the ground range for oblique data. The ground range for the sample data is 2060.00 km.

Type 2060.00

Finally, you will be prompted to input the data file containing the mid-point quasiparabolic electron density estimate. A sample file is provided called EDP01.INT.

Type edp01.int

The edp01.int has 3 columns and 3 rows. The first column corresponds to the E-layer data. The second column corresponds to the F1 layer data. The third corresponds to the F2 layer data. On the other hand the first row is the critical frequency. The second row is the semi-thickness and the third row is the base height.

Before the program proceeds, it will give you a chance to change parameters listed in the electron density file (in this case the sample file EDP01).

Type 0 for no change and 1 to change the parameters. To change the F2 layer, type 1. After the prompt, type the new parameters. The program is now running. It finds the updated quasiparabolic model for the E layer, F1 layer and F2 layer. The results are dumped to the screen. Also 8 files are generated. These files are: DEMO1.ed0 and DEMO1.iO0 containing the mid-point electron density profile and the group path of the sounding frequencies for the initial input.

DEMO1.ed1 and DEMO1.iO1 contain the mid-point edp and group paths at the indicated sounding frequencies after E layer inversion. DEMO2.ed2 and DEMO1.iO2 contain corresponding data after E and F1 layer inversion. DEMO1.ed3 and DEMO1.iO3 contain the corresponding data after E, F1 and F2 layer inversion.

Another executable file is gensyn.EXE. This program produces an oblique ionogram from a three layer quasiparabolic electron density profile file specified by the user. The ground range and frequency limits of the oblique ionogram are also selectable by the user.

To run this program, type gensyn after the prompt. You will be prompted the input the desired ground range. Type 2060.00, then you will be asked to input the mid-point electron density data file. Type DEMO1.ed3 (note that this file contains the optimal mid-point E, F1 and F2 layers).

The program will give you a chance to change the input parameter. Type 0 for no, 1 for yes. It will also give you a chance to change the frequency range data.

Then it will ask for the output file name, Type Sample.

The third executable field is plotsyn.EXE. This program plots both synthetic oblique ionograms and scaled oblique ionogram files.



To run this program type after the prompt plotsyn.

It will ask you to input the power threshold, type 0.0. Then it will prompt you to input the name of the file to be displayed type, Sample (output of gensyn program).

The program will display the starting frequency and the ending frequency and will ask you if you want to use these values. Enter 1 for yes and 0 for no. Type 1 and then it will ask you if you like to plot scaled points. Enter 1 for yes and 0 for no. Type 1.

Finally, the program will ask you if you would like to plot inversion data, type 1 for yes and 0 for no. Type 0.

Remark: The request for inversion data requires an ionogram inversion file such as DEMO1.iO\*.

Then an ionogram is produced. The horizontal axis is the frequency axis and the vertical axis is the ground range axis. The ground range axis has values between 2,000 km and 3,300 km. The horizontal axis is shown in 1 MHz steps.

The E layer is plotted in dark blue, 1 hop, and light blue 2 hop. The F1 layer light and dark red for 1 and 2 hop respectively. The F2 layer is green with the same light and dark 1 and 2 hop tagging.

C:\>d:

D:\>cd doris

D:\DORIS>ddir

DDIK for DOS 4.0 and 5.0, D. F. Kitrosser, 1992

Volume in drive D is MS-RAMDRIVE

Directory of D:\DORIS

.	(DIR)	04-14-92	8:26a	3	PLOTSYN	EXE	58882	05-03-91	2:13p	
..	(DIR)	04-14-92	8:26a	3	PLOTSYN	FOR	5383	05-03-91	2:13p	
DEM01		38515	04-13-92	2:52p	3	QPSUMHL	FOR	9142	06-26-91	4:46p
DORIS	DOC	3258	04-13-92	10:10a	3	QPSUMHL	OBJ	15386	07-23-91	4:16p
EDP01	INT	99	04-09-92	10:29a	3	ROOT	ED1	99	04-10-92	9:37a
GENEDP	FOR	1731	04-09-92	10:00a	3	ROOT	ED2	99	04-10-92	9:37a
GENSYN	EXE	45832	04-13-92	9:38a	3	ROOT	ED3	99	04-10-92	9:37a
GENSYN	FOR	4524	04-13-92	9:37a	7	ROOT	100	520	04-10-92	9:37a
GENSYN	OBJ	6476	04-13-92	9:38a	3	ROOT	101	520	04-10-92	9:37a
HOME	FOR	2354	04-07-92	2:45p	3	ROOT	102	504	04-10-92	9:37a
HOME	OBJ	3536	04-07-92	2:45p	3	ROOT	103	504	04-10-92	9:37a
OBL_INVR	EXE	56720	04-10-92	9:47a	3	SCLDATA		504	07-22-91	3:24p
OBL_INVR	FOR	13847	04-10-92	9:46a	3	SYTEST		47525	04-13-92	10:02a
OBL_INVR	OBJ	16742	04-10-92	9:47a	3					
Above display		324873	bytes in use		27	file(s)	594944	bytes free		

D:\DORIS>obl\_invr

input scaled trace data file

scldata

input name of output files

demol

input ground range for oblique data

2050.00

input midpoint electron density estimate data file

edp01.int

present qp model

E fc E rb E ym

F1 fc F1 rb F2 ym

F2 fc F1 rb F2 ym

4.00 90.00 20.00

6.00 120.00 70.00

10.50 210.00 160.00

do you want to change E layer yes=1 no=0

0

do you want to change F1 layer yes=1 no=0

0

do you want to change F2 layer yes=1 no=0

1

input F2 fc , F2 rb , F2 ym

10.3,210.0,160.0

Of 18 scaled points the initial estimate matched 15  
 With an average squared E group path error of 102.454  
 an average squared F1 group path error of 145.315  
 an average squared F2 group path error of 34.327

qp model updated during E layer processing

E fc	F1 fc	F2 fc
E ya	F1 ya	F2 ya
E rb	F1 rb	F2 rb
4.05	6.00	10.30
19.14	70.00	160.00
93.57	120.00	210.00

Of 18 scaled points the current estimate matched 15  
 With an average squared E group path error of 8.002  
 an average squared F1 group path error of 177.469  
 an average squared F2 group path error of 34.464

qp model updated during E layer processing

E fc	F1 fc	F2 fc
E ya	F1 ya	F2 ya
E rb	F1 rb	F2 rb
4.10	6.00	10.30
10.55	70.00	160.00
97.07	120.00	210.00

Of 18 scaled points the current estimate matched 16  
 With an average squared E group path error of 7.820  
 an average squared F1 group path error of 145.239  
 an average squared F2 group path error of 34.546

qp model after E layer processing

E fc	F1 fc	F2 fc
E ya	F1 ya	F2 ya
E rb	F1 rb	F2 rb
4.10	6.00	10.30
10.55	70.00	160.00
97.07	120.00	210.00

qp model updated during F1 layer processing

E fc	F1 fc	F2 fc
E ya	F1 ya	F2 ya
E rb	F1 rb	F2 rb
4.10	5.94	10.30
10.55	67.34	160.00
97.07	121.55	210.00

Of 18 scaled points the current estimate matched 17  
 With an average squared E group path error of 7.820  
 an average squared F1 group path error of 103.374  
 an average squared F2 group path error of 34.938

qp model updated during F1 layer processing

E fc	F1 fc	F2 fc
E ya	F1 ya	F2 ya
E rb	F1 rb	F2 rb
4.10	5.73	10.30
10.55	66.36	160.00
97.07	120.31	210.00

Of 16 scaled points the current estimate matched 16  
 With an average squared E group path error of 7.828  
 an average squared F1 group path error of 18.398  
 an average squared F2 group path error of 37.452

qp model updated during F1 layer processing

E fc	F1 fc	F2 fc
E ym	F1 ym	F2 ym
E rb	F1 rb	F2 rb

4.10	5.66	18.30
18.55	67.71	168.00
97.87	125.65	218.00

Of 16 scaled points the current estimate matched 16  
 With an average squared E group path error of 7.828  
 an average squared F1 group path error of 9.761  
 an average squared F2 group path error of 38.387

qp model updated during F1 layer processing

E fc	F1 fc	F2 fc
E ym	F1 ym	F2 ym
E rb	F1 rb	F2 rb

4.10	5.63	18.30
18.55	66.89	168.00
97.87	127.47	218.00

Of 16 scaled points the current estimate matched 16  
 With an average squared E group path error of 7.828  
 an average squared F1 group path error of 9.271  
 an average squared F2 group path error of 39.172

qp model updated during F1 layer processing

E fc	F1 fc	F2 fc
E ym	F1 ym	F2 ym
E rb	F1 rb	F2 rb

4.10	5.72	18.30
18.55	68.14	168.00
97.87	138.63	218.00

Of 16 scaled points the current estimate matched 16  
 With an average squared E group path error of 7.628  
 an average squared F1 group path error of 7.554  
 an average squared F2 group path error of 38.548

qp model updated during F1 layer processing

E fc	F1 fc	F2 fc
E ym	F1 ym	F2 ym
E rb	F1 rb	F2 rb

4.10	5.76	18.30
18.55	67.51	168.00
97.87	133.71	218.00

Of 16 scaled points the current estimate matched 16  
 With an average squared E group path error of 7.628  
 an average squared F1 group path error of 6.916  
 an average squared F2 group path error of 38.586

qp model updated during F1 layer processing

E fc	F1 fc	F2 fc
E ym	F1 ym	F2 ym
E rb	F1 rb	F2 rb

4.10	5.73	18.30
18.55	69.23	168.00
97.87	138.97	218.00

Of 18 scaled points the current estimate matched 18  
 With an average squared E group path error of 7.828  
 an average squared F1 group path error of 6.915  
 an average squared F2 group path error of 38.484  
 qp model updated during F1 layer processing

E fc	F1 fc	F2 fc
E ym	F1 ym	F2 ym
E rb	F1 rb	F2 rb
4.18	5.88	18.38
18.55	69.51	168.08
97.87	134.88	218.88

Of 18 scaled points the current estimate matched 18  
 With an average squared E group path error of 7.828  
 an average squared F1 group path error of 6.534  
 an average squared F2 group path error of 38.318  
 qp model updated during F1 layer processing

E fc	F1 fc	F2 fc
E ym	F1 ym	F2 ym
E rb	F1 rb	F2 rb
4.18	5.74	18.38
18.55	68.87	168.88
97.87	133.98	218.88

Of 18 scaled points the current estimate matched 18  
 With an average squared E group path error of 7.828  
 an average squared F1 group path error of 5.419  
 an average squared F2 group path error of 38.864  
 qp model after E and F1 layer processing

E fc	F1 fc	F2 fc
E ym	F1 ym	F2 ym
E rb	F1 rb	F2 rb
4.18	5.74	18.38
18.55	68.87	168.88
97.87	133.98	218.88

qp model updated during F2 layer processing

E fc	F1 fc	F2 fc
E ym	F1 ym	F2 ym
E rb	F1 rb	F2 rb
4.18	5.74	18.16
18.55	68.87	166.91
97.87	133.98	209.95

Of 18 scaled points the current estimate matched 18  
 With an average squared E group path error of 7.828  
 an average squared F1 group path error of 5.419  
 an average squared F2 group path error of 19.386  
 qp model updated during F2 layer processing

E fc	F1 fc	F2 fc
E ym	F1 ym	F2 ym
E rb	F1 rb	F2 rb
4.18	5.74	18.89
18.55	68.87	161.75
97.87	133.98	214.98

Of 18 scaled points the current estimate matched 18  
 With an average squared E group path error of 7.828  
 an average squared F1 group path error of 5.419  
 an average squared F2 group path error of 18.912

qp model updated during F2 layer procesing

E fc	F1 fc	F2 fc
E ym	F1 ym	F2 ym
E rb	F1 rb	F2 rb

4.18	5.74	18.88
18.55	68.87	166.62
97.87	133.98	218.44

Of 18 scaled points the current estimate matched 18  
 With an average squared E group path error of 7.828  
 an average squared F1 group path error of 5.419  
 an average squared F2 group path error of 6.658

qp model updated during F2 layer procesing

E fc	F1 fc	F2 fc
E ym	F1 ym	F2 ym
E rb	F1 rb	F2 rb

4.18	5.74	18.87
18.55	68.87	172.26
97.87	133.98	289.43

Of 18 scaled points the current estimate matched 18  
 With an average squared E group path error of 7.828  
 an average squared F1 group path error of 5.419  
 an average squared F2 group path error of 7.682

qp model updated during F2 layer procesing

E fc	F1 fc	F2 fc
E ym	F1 ym	F2 ym
E rb	F1 rb	F2 rb

4.18	5.74	18.13
18.55	68.87	169.58
97.87	133.98	213.58

Of 18 scaled points the current estimate matched 18  
 With an average squared E group path error of 7.828  
 an average squared F1 group path error of 5.419  
 an average squared F2 group path error of 6.674

qp model after E F1 and F2 layer processing

E fc	F1 fc	F2 fc
E ym	F1 ym	F2 ym
E rb	F1 rb	F2 rb

4.18	5.74	18.13
18.55	68.87	169.58
97.87	133.98	213.58

```

E:\DORIS>gensyn
input desired ground range
2036.0
input midpoint electron density data file
demol.ed3
present qp model
E fc      E rb      E ya
F1 fc      F1 rb      F2 ya
F2 fc      F1 rb      F2 ya
    4.10      97.87      18.55
    5.74      133.90      68.87
    18.13      213.58      169.50
do you want to change E layer yes=1 no=0
0
do you want to change F1 layer yes=1 no=0
0
do you want to change F2 layer yes=1 no=0
0
present frequency range data  fo,dltf,fmax
    5.000      .100      20.000
do you want to change these values yes=1 no=0
0
generating oblique ionogram
    5.0000000000000000  1.000000014901161E-001  20.0000000000000000
input name of output file
sample

```

```

E:\DORIS>
E:\DORIS>plotsyn
input power threshold
6.0
input name of file to be displayed
sample
    4.100000      5.740000      18.130000
    18.550000      68.670000      169.500000
    57.870000      133.900000      213.500000
fmin =      5.000000fmax =      20.000000
do you want to use these values 1=yes 0=no
1
do you want to plot scaled points 1=yes 0=no
1
input name of scaled point file
scldata
do you want to plot inversion data 1=yes 0=no
0

```